forests

MDPI

Communication

Annual Variations in Norway Spruce Xylem Studied Using Infrared Micro-spectroscopy

Weiwei Huang [1,2,*], Nanna Bjerregaard Pedersen [2,3], Maria Fredriksson [2,4] and Lisbeth Garbrecht Thygesen [2]

1 Collaborative Innovation Center of Sustainable Forestry in Southern China of Jiangsu Province, Bamboo Research Institute, Nanjing Forestry University, Nanjing 210037, China
2 Department of Geosciences and Natural Resource Management, University of Copenhagen, Rolighedsvej 23, DK-1958 Frederiksberg C, Denmark; nbje@kadk.dk (N.B.P.); maria.fredriksson@byggtek.lth.se (M.F.); lgt@ign.ku.dk (L.G.T.)
3 School of Conservation, The Royal Danish Academy of Fine Arts Schools of Architecture, Design and Conservation, Esplanaden 34, DK-1263 Copenhagen K, Denmark
4 Division of Building Materials, Lund University, P.O. Box 118, SE-221 00 Lund, Sweden
* Correspondence: wh@njfu.edu.cn; Tel.: +86-25-8542-7231

Received: 11 December 2018; Accepted: 14 February 2019; Published: 15 February 2019



Abstract: In temperate environments, ring width, cell size and cell wall thickness within the xylem of trees are known to be affected by climate conditions. Less is known about the effect of climate conditions on the chemical characteristics of the xylem, which are important for the susceptibility of the tissue towards fungal infections as well as for the degradability of the material within the forest ecosystem. We explored the use of infrared microspectroscopy to investigate the possible effects of temperature and drought on the relative amount of cell wall biopolymers, i.e. the ratios between cellulose, hemicellulose and lignin in the earlywood xylem cell walls of Norway spruce (*Picea abies* (L.) Karst.) in temperate forests. Drought and warm temperatures were significantly correlated to the hemicellulose to lignin ratio of the earlywood formed the following year, perhaps due to a reduced amount of stored resources being available for xylem formation.

Keywords: dendroecology; biopolymer composition; climate; drought; infrared microspectroscopy; temperature; xylem plasticity

1. Introduction

Current climate scenarios for northern Europe in the later part of the 21th century predict longer growing seasons, dryer summers and warmer autumns [1,2]. It is well-known that spring and/or summer droughts affect conifer tree growth negatively in a temperate climate [3–7], and that cambium phenology is related to climate [8,9]. It is also known that xylem characteristics, like for example cell size and cell wall thickness, are related to ecological factors, of which climate is one [10–18]. However, less is known about the possible effects of climate on the biopolymer composition of the xylem formed. Xylem cell dimensions and cell wall thicknesses affect physical wood properties such as density [19] as well as tree physiology via e.g. water conductance [20]. Cell wall chemistry on the other hand is important for the biodegradability of the wood, as for example a high lignin content generally correlates to high recalcitrance of plant biomass [21]. Based on this knowledge, it is possible that climate indirectly might affect both the susceptibility of the living tree to fungal attacks as well as the biodegradability of dead wood within the forest ecosystem. We consequently find it relevant to study the possible relations between climate and xylem cell wall biopolymer composition.

In temperate conifers, the chemical composition differs between earlywood and latewood: Earlywood generally contains more lignin and less cellulose and hemicellulose than latewood expressed as

weight percent of dried wood [22,23]. This is an effect of differences in xylem structure, where earlywood consists of larger and more thin-walled cells, and thus contains more lignin-rich middle lamella per gram of dry matter. The difference in cell wall chemistry between earlywood and latewood implies that the amounts of earlywood and latewood present within each ring may give rise to confounding effects rather than climate signals only in studies where the chemical composition of whole tree rings were analyzed. Therefore, microspectroscopy appears to be a good alternative in studies where the aim is to clarify the effects of temperature and precipitation on xylem cell wall composition, as these techniques offer the spatial resolution required [24]. This approach seems not to have been attempted until recently [25]. Chemical imaging studies of conifer tracheid secondary cell wall have shown significantly higher relative lignin content in earlywood than latewood [26,27], emphasizing the need to study these two wood types separately in order to minimize the noise when attempting to link cell wall chemistry to climate signal.

In the present work we used Fourier transform infrared (FT-IR) microspectroscopy to test the hypothesis that drought and temperature of the current and preceding growth seasons affect the chemical composition of earlywood from *P. abies*. Studies of this species grown under temperate conditions have indicated that a warm autumn is associated with reduced tree vitality the following year [7,28], perhaps due to a lower amount of non-structural carbohydrates being stored over the winter. Presumably this signal would be strongest in the earlywood, and therefore, FT-IR microspectroscopy was applied to track variations in relative amounts of cellulose, hemicellulose and lignin in earlywood cell walls.

2. Material and Methods

2.1. Experimental Site and Xylem Samples

The wood discs used as sample material came from an experimental site in a plantation forest in Frederiksborg, Denmark (latitude 55°57′21.3″ N, longitude 12°21′14.1″ E) established in 1964 with a mean annual temperature of 8.2 °C and an annual precipitation of 605 mm (period 1961–2012) [29]. The former use of the area was as cropland and the soil texture is sandy loam with a subsoil clay content of 23% [30]. The field trial includes 10 non-native conifer species and two native broadleaved species. Stem discs from 1.3 m above ground were acquired during the winter 2012–2013 from three *P. abies* co-dominant trees by thinning. The discs were oven dried at 103 °C prior to analysis. For further information, please see [7].

2.2. Temperature and Drought Data

Average monthly temperature, precipitation and potential evapotranspiration were obtained from the 0.5° grid observational data from CRU TS v.3.22 from 1997 to 2012 [31]. Monthly drought index (*DI*) was estimated as monthly precipitation minus monthly potential evapotranspiration [32,33]. Low *DI* corresponds to dry conditions.

2.3. Silviscan Density Measurements and Infrared Microspectroscopy

Two adjacent radial strips covering pith to bark and approximately 5 mm wide were cut from each of the three discs. One strip was characterized by use of the instrument Silviscan [34]. Using this instrument, density was measured by X-ray densitometry with a spatial resolution of 25 μm. Within each ring, positions having a wood density within 0–20% of the span from minimum to maximum wood density recorded for the ring was assigned to earlywood, the part within 80–100% of the span was assigned to latewood, and the remaining part was assigned to transition wood [35]. The Silviscan measurement also included micrographs of the cross sectional area and automatic image analysis resulting in estimates of earlywood width (EW), tangential and radial lumen diameter (LUM_t and LUM_r) and cell wall thicknesses (CWT) for the three different wood types of each ring (for further information on the Silviscan equipment please refer to Evans & Ilic [34]).

The second radial strip was used for FT-IR micro-spectroscopy measurements. Subsamples containing three to six tree rings each (maximum subsample width of 10 mm) from the outermost 15 to 17 tree rings were isolated using a razor blade. A total of 33 sapwood tree rings were included, covering the calendar years 1997–2012 in three different trees. The subsamples were vacuum-saturated in water and cut into nominally 20-µm thick specimens from the radial face using a sliding microtome. Obtaining transmission spectra in the radial direction is unusual but ensured that each individual spectrum expressed a mixture of the cell wall layers present within each cell. The specimens were air-dried on glass slides for at least 1 h and mounted on cardboard frames for IR transmission measurements. A visual survey image (10.000 × 10.000 µm) and one IR image were recorded for each specimen using a Perkin-Elmer Spectrum Spotlight 400 FT-IR microscope (Perkin-Elmer, Waltham, Massachusetts, USA) equipped with a MCT detector. A new background (in air) was taken before each image was recorded with the settings: 8 cm^{-1}, 15 scans, 4000–720 cm^{-1}, interferometer speed 1 cm/s, and spatial resolution of 25 × 25 µm (one pixel). The settings used for imaging were the same, except that the number of scans per spectrum was reduced to eight. IR images, four lines in height and covering the whole width of the specimen, were captured (Figure 1). All IR images were 4 × 25 = 100 µm in height, while the width varied depending on the total width of the tree rings included in the specimen.

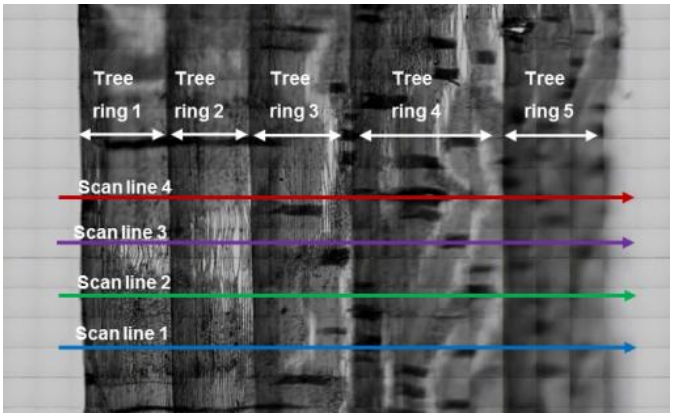

Figure 1. Visual survey image of Norway spruce subsample with colored arrows showing the principle spatial position of the four scan lines recorded on each of the investigated subsamples.

All spectra from all subsamples and all four scanlines were manually inspected. This was done to verify the quality of the spectra, to validate that the four spectra from the four individual scanlines could be regarded as replicates (Figure 1), and to locate the tree ring boarders in the subsamples. The individual spectra were manually assigned to the individual tree rings of the wood samples by measurement of the tree ring widths in the visual survey images using GIMP 2.8 (GNU Image Manipulation Program, free software available from gimp.org/downloads/). In addition, the spectra were used to locate the tree ring borders; as the spectra clearly showed a consistent shift in band pattern at 1000–1100 cm^{-1} at the tree ring border. The spectra were assigned to earlywood, transition wood or latewood based on the Silviscan density measurements, and only the earlywood spectra were included in the study [35]. In approximately half of the analyzed tree rings, thin patches in the specimens had resulted in spectra of low quality with signals from air rather than from wood. In order to make sure that all included radial positions were represented by four spectra, all four spectra obtained for the same radial position were excluded in case one or more spectra were of low quality.

To observe quantitative changes in xylem cell wall biopolymer composition between the studied annual rings, ratios of peak areas from the FT-IR spectra were evaluated. The lignin polymer contains a high number of aromatic functional groups not present in carbohydrates [23,36]. The FT-IR absorption band at 1508 cm^{-1} is assigned to aromatic skeletal vibrations, and the band can thereby be directly

assigned to the lignin polymer with no contributions from carbohydrates in wood and other types of plant material [37].

It is by far more complex to assign FT-IR bands to the structural carbohydrates cellulose and hemicellulose present in the wood cell walls since both polymers are composed of monomer units of aldoses and ketoses (monosaccharides). The band at 1104 cm^{-1} is assigned to ring asymmetric valence vibration in polysaccharides [38,39] and the band does thereby represent contributions from both cellulose and hemicellulose (holocellulose). The band at 1056 cm^{-1} is assigned to C-O valence vibration mainly from C_3-OH in six membered pyranose rings [40]. All glucose units in cellulose have this C_3-OH valence vibration, whereas the most abundant hemicellulose in softwood, galactoglucomannan, lack this vibration in some mannose units as the C_3 is partly substituted by acetyl groups. The second most abundant hemicellulose in softwood is arabino-4-O-methylglucuronoxylan. This type of hemicellulose does also lack monosaccharide units with C_3-OH valence vibration as arabinose form a five membered furanose ring. In addition, the arabinose units are linked to the xylan backbone at the C_3 position [41]. In conclusion, the 1056 cm^{-1} vibration band is not specific for cellulose but the band intensity should be more influenced by quantitative change in cellulose than hemicellulose.

Hemicellulose differs from cellulose and lignin by containing unconjugated carbonyl groups in acetyl groups in softwood galactoglucomannan and carboxylic acid functional groups in methylglucuronic acid side groups in xylan [42]. In addition, unconjugated ester groups are present in lignin-carbohydrate complexes formed between carboxylic acid groups in methylglucuronic acid side chain of xylan and γ-hydroxyl on the side chain of lignin monomer units [42]. The absorption band at 1732 cm^{-1} is assigned to C=O stretch in unconjugated carbonyl groups [38,43]. The band at 1732 cm^{-1} can therefore be assigned to hemicellulose with no contributions from cellulose or lignin. However, an important point is that changes in relative band intensity cannot be used as conclusive evidence for changes in the amount of the hemicellulose polymer backbone unless it is assumed that the degree of acetylation in galactoglucomannan and the relative amount of methylglucuronic acid in xylan is unchanged. The degree of acetylation in galactoglucomannan is in the range 4.3–8.8% for different softwood species, whereas the degree of methylglucuronic acid attached to the xylose backbone is in the range 16–23% [23].

The peak area ratios used to evaluate the quantitative changes in xylem cell wall biopolymer composition in this study were 1104 cm^{-1}/1508 cm^{-1} (henceforth denoted 1104/1508) to evaluate the holocellulose/lignin ratio, 1104 cm^{-1}/1732 cm^{-1} (henceforth denoted 1104/1732) to evaluate the holocellulose/hemicellulose ratio, 1732 cm^{-1}/1508 cm^{-1} (henceforth denoted 1732/1508) evaluate the hemicellulose/lignin ratio, and 1056 cm^{-1}/1508 cm^{-1} (henceforth denoted 1056/1508) to evaluate the cellulose/lignin ratio (Table 1). The four ratios of the peak areas were computed based on the raw absorbance spectra; the four replica scanlines were not averaged. Peak areas were calculated using an individual linear baseline for each peak (Matlab R2014a, MathWorks).

Table 1. Assignment of the four absorbance bands used for calculating five band area ratios to determine quantitative compositional changes between annual rings.

Band Position [cm^{-1}]	Wood Polymer	Assignment [1]
1508	Lignin	Aromatic skeletal vibrations
1104	Holocellulose	Ring asymmetric valence vibration in polysaccharides
1056	Cellulose	C-O valence vibration mainly from C_3-OH in six membered pyranose rings (present in all cellulose monomers, lacking in some hemicellulose monomers)
1732	Hemicellulose	C=O stretch in unconjugated carbonyl groups of carbohydrate origin (side chain acetylation in mannan, carboxylic acid side chain in xylan, and ester groups in lignin-carbohydrate complexes)

[1] From Fackler et al. [39], Faix [37], Marchessault [43], Maréchal & Chanzy [40], and Schwanninger et al. [38].

2.4. Data Analysis

IR peak area ratios (1056/1508, 1104/1508, 1104/1732 and 1732/1508) were calculated for all spectra selected after the previously described quality control, and means were calculated for each ring from each tree. In addition, the mean value for each year (i.e., mean of the three trees) was calculated. The relationship between peak area ratios and cell dimensions were calculated based on Pearson's correlation both on tree level and across the three sampled trees. Plots were used to check significant linear relationships. The correlation between the mean peak area ratios and the monthly mean temperature as well as the cumulated *DI* were determined by calculation of Pearson's correlation coefficients. The correlations were determined both for the monthly average temperature in the previous year (June–December) and the current year (January–August) or the cumulated *DI* indices for different consecutive periods from March to August (*DI*3–*DI*8) in current-year and March to September (*DI*3–*DI*9) in previous-year. Finally, the previous and current year drought indices and monthly temperatures with significant ($p < 0.05$) correlations with the peak area ratios were identified. When calculating correlations across the three trees, only years for which IR data had been obtained for all three trees were included. The plots and MIXED procedure of the statistical software SAS were used to determine whether the relationships were linear [44,45]. The model used was defined as:

$$Peak\ ratio_j = \mu + \beta_n X_{nj} + \alpha_n X_{nj}^2 + e_j \quad (1)$$

where $Peak\ ratio_j$ is the mean IR peak ratio for each tree or the mean for the three sampled trees and year j, μ is the general mean, X_{nj} is the climate variable n in year j (i.e., the climatic variables significantly correlated with the IR peak ratio), β_n is the regression coefficients for climate variable n, X_{nj}^2 is the squared climate variable n in year j, α_n is regression coefficients for squared climate variable n, e_j is the residual.

3. Results

Significant correlations between temperature and IR peak ratios and between *DI* and IR peak ratios were identified (Table 2).

Regarding temperature, significant correlations across all trees were found for the 1732/1508 peak ratio (hemicellulose/lignin) and 1104/1508 (holocellulose/lignin). The correlation was positive between ratio 1732/1508 and the July, September and November temperatures of the previous year, indicating a higher hemicellulose content relative to lignin in a year following a warm summer or autumn. The correlation was positive between the 1104/1508 peak ratio and the June temperature of the current year, indicating a higher holocellulose content relative to lignin in years with a warm summer.

The 1732/1508 ratio (hemicellulose/lignin) showed a significant negative correlation with the *DI* in the previous-year growth season across all trees, indicating that drought was related to a higher hemicellulose to lignin ratio within the earlywood formed the next year. For one of the trees, a negative correlation between the 1732/1508 ratio and current-year growing season *DI* was also found, again indicating a correlation between drought and lower lignin content compared to hemicellulose. However, contrasting results were found for the 1056/1508 ratio (cellulose/lignin), which showed a weak negative effect of current summer *DI* for one tree and a positive influence of previous growing season *DI* for another tree.

Table 2. List of significant correlations between IR peak ratios and monthly temperature or drought index (*DI*).

	Peak Ratio	Tree No.	Number of Years [a]	Prev. or Curr. Year [b]	Month(s)	Coefficient	*p*-Value
Influence of temperature							
Cellulose/lignin	1056/1508	N1	11	curr.	Jun	0.70	0.016
		N2	10	prev.	Jul	−0.64	0.047
		N2	10	curr.	Mar	−0.69	0.026
		N3	12	prev.	Sep	0.59	0.045
		all trees	6	ns	ns	ns	ns
Holocellulose/lignin	1104/1508	N1	11	curr.	Jun	0.74	0.009
		N2	10	prev.	Jul	−0.64	0.048
		N3	12	prev.	Sep	0.64	0.024
		N3	12	curr.	Jul	−0.59	0.042
		all trees	6	curr.	Jun	0.84	0.037
Holocellulose/hemicellulose	1104/1732	N1	11	curr.	Jun	0.64	0.036
		N2	10	curr.	Mar	−0.67	0.034
		N3	12	prev.	Sep	0.68	0.015
		all trees	6	ns	ns	ns	ns
Hemicellulose/lignin	1732/1508	N1	11	ns	ns	ns	ns
		N2	10	curr.	Mar	0.63	0.049
		N3	12	curr.	Feb	0.64	0.026
		N3	12	curr.	May	0.59	0.043
		all trees	6	prev.	Jul	0.86	0.027
		all trees	6	prev.	Sep	0.84	0.036
		all trees	6	prev.	Nov	0.82	0.043
Influence of DI							
Cellulose/lignin	1056/1508	N2	10	curr.	Jun–Aug	−0.64	0.046
		N3	12	prev.	Mar–Jun	0.61	0.037
		all trees	6	ns	ns	ns	ns
Holocellulose/lignin	1104/1508	all trees	6	curr.	Mar–Jun	0.82	0.046
Hemicellulose/lignin	1732/1508	N3	12	curr.	Apr–Jun	−0.67	0.016
		N3	12	curr.	May–Jun	−0.69	0.013
		all trees	6	prev.	Mar–Jul	−0.96	0.003
		all trees	6	prev.	Apr–Jul	−0.95	0.004
		all trees	6	prev.	Jun–Jul	−0.88	0.021
		all trees	6	prev.	May–Jul	−0.86	0.028

[a] Number of years where spectra were included in the analysis. The calendar years were: Tree no. N1, year 1997, 2000, 2001, 2003, 2004, 2005, 2006, 2007, 2009, 2010 and 2012; Tree no. N2, year 1998, 2003, 2005, 2006, 2007, 2008, 2009, 2010, 2011 and 2012; Tree no. N3, year 1997, 1999, 2000, 2002, 2003, 2005, 2006, 2007, 2008, 2010, 2011 and 2012; all trees, year 2003, 2005, 2006, 2007, 2010 and 2012. [b] curr. = current year climate; prev. = previous year climate. ns: non-significant correlation ($p > 0.05$).

The relationships found between IR peak ratios and cell dimensions are shown in Table 3. The mean 1104/1732 ratio (holocellulose/hemicellulose) and 1104/1508 (holocellulose/lignin) across the three sampled trees were positively correlated to the earlywood width ($p < 0.05$); however, the significant relationship found for 1104/1508 was an artefact due to an outlier. When including all trees, the radial lumen diameter (LUM_r) showed a negative relationship with 1056/1508 (cellulose/lignin), 1104/1508 (holocellulose/lignin), and 1104/1732 (holocellulose/hemicellulose). The 1732/1508 ratio (hemicellulose/lignin) did not show any significant relationship with any cell dimensions across all three trees.

Table 3. Relationship between IR peak ratios and cell dimensions, i.e., earlywood width (EW), wood density (density), tangential lumen diameter (LUM_t), radial lumen diameter (LUM_r) and cell wall thickness (CWT).

Peak Ratio	Tree No.	Number of Years [a]	EW	Density	LUM_t	LUM_r	CWT
1056/1508 (Cellulose/lignin)	N1	11	ns	ns	ns	ns	ns
	N2	10	ns	ns	ns	ns	ns
	N3	12	ns	ns	ns	ns	ns
	all trees	6	ns	ns	ns	**−0.82** *	ns
1104/1508 (holocellulose/lignin)	N1	11	ns	ns	ns	ns	ns
	N2	10	**0.65** *	ns	ns	ns	ns
	N3	12	ns	ns	ns	ns	ns
	all trees	6	**0.85** *	ns	ns	**−0.85** *	ns
1104/1732 (Hollocellulose/hemicellulose)	N1	11	ns	ns	ns	ns	ns
	N2	10	ns	ns	ns	ns	ns
	N3	12	ns	ns	ns	ns	ns
	all trees	6	**0.97** **	ns	ns	**−0.83** *	ns
1732/1508 (Hemicellulose/lignin)	N1	11	ns	ns	ns	**0.64** *	ns
	N2	10	ns	ns	ns	ns	ns
	N3	12	ns	ns	ns	ns	**0.58** *
	all trees	6	ns	ns	ns	ns	ns

[a] Number of years for which spectra were analyzed (please refer to Table 2 for a list of calendar years). The significance of the Pearson's correlation coefficients are indexed with* if $p < 0.05$, ** if $p < 0.01$, and *** if $p < 0.001$.

4. Discussion

Our finding that temperature stress is related to lignin content within the xylem cell walls agrees with some but not all earlier studies, albeit no study exactly like the present one could be found. Gindl et al. [46] found, based on data from 50 tree rings from five *Picea abies* (L.) Karst trees, that the lignin concentration in the secondary cell wall layer (S2) of the terminal latewood tracheids was lower during years with relatively lower temperatures in September–October. For another *P. abies* tree, Gindl & Grabner [47] found that the lignin concentration was markedly reduced in all latewood tracheids formed in a year with abnormally low temperatures in September to October. On the other hand Kilpeläinen et al. [48] found that the xylem (earlywood and latewood was not separated) produced in eight 15-year-old *Pinus sylvestris* (L.) trees grown under elevated temperatures had higher relative lignin content and lower relative hemicellulose content than in trees exposed to ambient temperatures. However, in a later study, including eight 20-year-old *P. sylvestris* trees grown under elevated temperatures, no significant effects of higher temperature on the relative content of cellulose, lignin and hemicellulose were found, but the relative content of acetone-soluble extractives was lower [49]. In a similar experiment, including six *P. abies* trees grown under elevated temperatures, Kostiainen et al. [50] found no effect on the relative content of lignin and of α-cellulose in the xylem (earlywood and latewood was not separated), but the relative content of extractable and soluble sugars decreased for the trees exposed to elevated temperatures.

Regarding our findings on the relation between drought stress and relative lignin content, a point to consider is that the lignin content is higher in the middle lamella and in cell corners than in the secondary cell wall. The recorded mean 1732/1508 ratio can therefore be expected to decrease if the earlywood radial tracheid diameter is reduced as more of the transmission spectra reflect lignin-rich regions (the spectra were obtained in the radial direction, see Figure 1). However, no significant relationship was found between the 1732/1508 ratio and cell dimensions when including all three sampled trees (Table 3). This indicates that the observed correlations between drought and warm

weather and decreased lignin content relative to hemicellulose most likely is due to chemical changes in the cell wall material and not due to anatomical differences. Donaldson [51] found poorly lignified middle lamella and outer secondary walls in *Pinus radiata* (D. Don) specimens. These abnormalities were assumed to be the result of frequent water stress and possibly associated with nutritional stress. Nanayakkara et al. [52], on the other hand, found also for *P. radiata*, that drought stress significantly increases the relative content of arabinose, galactose, glucose and xylose in normal wood of one-year old plants. In a more general review on the effect of abiotic stresses on lignins, Cabane et al. [53] concluded that abiotic stress affects lignin biogenesis pathways.

The results of the current study indicate that climate might have an effect on tree growth not only via ring widths and cell dimensions, but also via xylem cell wall composition. We suggest that this aspect of tree growth also be included when studying the interrelations between xylem characteristics and growth conditions.

5. Conclusions

Our results indicate that warm summers and drought stress are related to the formation of earlywood xylem containing relatively less lignin than would otherwise be the case. The lower lignin content suggests that the wood formed is more susceptible to fungal degradation, both in the living tree and as dead wood. If these climate conditions become prevailing, the relation found could potentially contribute to a higher risk of forest stand decline and a speeding up of the carbon cycle within temperate forest ecosystems. However, the study is based on a very limited number of trees from only one location and results need to be confirmed by additional studies including more sites, more species and more trees. Furthermore, different types of models [54], i.e., not merely linear ones, could be explored when attempting to link climate and infrared peak ratios. Also, even though reduced lignin content is generally known to reduce recalcitrance in plant biomass, this notion needs to be confirmed to also be the case in this particular situation.

Author Contributions: Conceptualization, L.G.T.; formal Analysis, W.H., N.B.P. and L.G.T.; investigation, W.H. and L.G.T.; writing—original draft preparation, W.H., N.B.P., M.F. and L.G.T.; writing—review & editing, W.H., N.B.P., M.F. and L.G.T.; supervision, L.G.T.; funding acquisition, W.H. and L.G.T.

Funding: This research was funded by Gluds Legat, Tree4future, China Scholarship Council (CSC, No. 201306910037) and the Natural Science Foundation of the Jiangsu Higher Education Institutions of China (No. 18KJB220005).

Acknowledgments: The authors thank Innventia (Stockholm) to make the Silviscan measurements possible.

Conflicts of Interest: The authors declare no conflict of interest.

References

1. Bates, B.C.; Kundzewicz, Z.W.; Wu, S.; Palutikof, J.P. *Climate Change and Water*; Technical Paper of the Intergovernmental Panel on Climate Change; IPCC Secretariat: Geneva, Switzerland, 2008.
2. IPCC. *Climate Change 2013: The Physical Science Basis. Working Group I: Contribution to the Fifth Assessment Report of the Intergovernmental Panel on Climate Change*; Stocker, T.F., Qin, D., Plattner, G.K., Tignor, M.M.B., Allen, S.K., Boschung, J., Nauels, A., Xia, Y., Bex, V., Midgley, P.M., Eds.; Cambridge University Press: Cambridge, UK; New York, NY, USA, 2013; 1535p.
3. Van Mantgem, P.J.; Stephenson, N.L. Apparent climatically induced increase of tree mortality rates in a temperate forest. *Ecol. Lett.* **2007**, *10*, 909–916. [CrossRef] [PubMed]
4. Allen, C.D.; Macalady, A.K.; Chenchouni, H.; Bachelet, D.; McDowell, N.; Vennetier, M.; Kitzberger, T.; Rigling, A.; Breshears, D.D.; Hogg, E.H.; et al. A global overview of drought and heat-induced tree mortality reveals emerging climate change risks for forests. *For. Ecol. Manag.* **2010**, *259*, 660–684. [CrossRef]
5. Sohar, K.; Helama, S.; Läänelaid, A.; Raisio, J.; Tuomenvirta, H. Oak decline in a southern Finnish forest as affected by a drought sequence. *Geochronometria* **2013**, *41*, 92–103. [CrossRef]
6. Rosner, S.; Světlík, J.; Andreassen, K.; Børja, I.; Dalsgaard, L.; Evans, R.; Luss, S.; Tveito, O.E.; Solberg, S. Novel hydraulic vulnerability proxies for a boreal conifer species reveal that opportunists may have lower survival prospects under extreme climatic events. *Front. Plant Sci.* **2016**, *7*, 831. [CrossRef] [PubMed]

7. Huang, W.; Fonti, P.; Larsen, J.B.; Ræbild, A.; Callesen, I.; Pedersen, N.B.; Hansen, J.K. Projecting tree-growth responses into future climate: A study case from a Danish-wide common garden. *Agric. For. Meteorol.* **2017**, *247*, 240–251. [CrossRef]
8. Rossi, S.; Morin, H.; Deslauriers, A.; Plourde, P.-Y. Predicting xylem phenology in black spruce under climate warming. *Glob. Chang. Biol.* **2011**, *17*, 614–625. [CrossRef]
9. Rossi, S.; Morin, H.; Deslauriers, A. Causes and correlations in cambium phenology: Towards an integrated framework of xylogenesis. *J. Exp. Bot.* **2012**, *63*, 2117–2126. [CrossRef]
10. Park, Y.I.; Spiecker, H. Variations in the tree-ring structure of Norway spruce (*Picea abies*) under contrasting climates. *Dendrochronologia* **2005**, *23*, 93–104. [CrossRef]
11. Fernandez, M.E.; Gyenge, J.E.; de Urquiza, M.M.; Varela, S. Adaptability to climate change in forestry species: Drought effects on growth and wood anatomy of ponderosa pines growing at different competition levels. *For. Syst.* **2012**, *21*, 162–173. [CrossRef]
12. Bryukhanova, M.; Fonti, P. Xylem plasticity allows rapid hydraulic adjustment to annual climatic variability. *Trees Struct. Funct.* **2013**, *27*, 485–496. [CrossRef]
13. Fonti, P.; Heller, O.; Cherubini, P.; Rigling, A.; Arend, M. Wood anatomical responses of oak saplings exposed to air warming and soil drought. *Plant Biol.* **2013**, *15*, 210–219. [CrossRef] [PubMed]
14. Olano, J.M.; Almería, I.; Eugenio, M.; von Arx, G. Under pressure: How a Mediterranean high-mountain forb coordinates growth and hydraulic xylem anatomy in response to temperature and water constraints. *Funct. Ecol.* **2013**, *27*, 1295–1303. [CrossRef]
15. Xu, J.; Lu, J.; Bao, F.; Evans, R.; Downes, G.M. Climate response of cell characteristics in tree rings of *Picea crassifolia*. *Holzforschung* **2013**, *67*, 217–225. [CrossRef]
16. Fonti, P.; Babushkina, E.A. Tracheid anatomical responses to climate in a forest-steppe in Southern Siberia. *Dendrochronologia* **2016**, *39*, 32–41. [CrossRef]
17. Cuny, H.E.; Rathgeber, C.B.K. Xylogenesis: Coniferous trees of temperate forests are listening to the climate tale during the growing season but only remember the last words! *Plant Physiol.* **2016**, *171*, 306–317. [CrossRef] [PubMed]
18. Krause, C.; Rossi, S.; Thibeault-Martel, M.; Plourde, P-Y. Relationships of climate and cell features in stems and roots of black spruce and balsam fir. *Ann. For. Sci.* **2010**, *67*, 402. [CrossRef]
19. Schmulsky, R.; Jones, P.D. *Forest Products and Wood Science an Introduction*, 6th ed.; Wiley-Blackwell: Chichester, UK, 2011.
20. Sperry, J.S.; Hacke, U.G.; Pittermann, J. Size and function in conifer tracheids and angiosperm vessels. *Am. J. Bot.* **2006**, *93*, 1490–1500. [CrossRef]
21. Zhao, X.; Zhang, L.; Liu, D. Biomass recalcitrance. Part I: The chemical compositions and physical structures affecting the enzymatic hydrolysis of lignocellulose. *Biofuels Bioprod. Bioref.* **2012**, *6*, 465–482. [CrossRef]
22. Bertaud, F.; Holmbom, B. Chemical composition of earlywood and latewood in Norway spruce heartwood, sapwood and transition zone wood. *Wood Sci. Technol.* **2004**, *38*, 245–256. [CrossRef]
23. Fengel, D.; Wegener, G. *Wood: Chemistry, Ultrastructure, Reactions*; Kessel Verlag: Remangen, Germany, 2003.
24. Fackler, K.; Thygesen, L.G. Microspectroscopy as applied to the study of wood molecular structure. *Wood Sci. Technol.* **2013**, *47*, 203–222. [CrossRef]
25. Tyutkova, E.A.; Loskutov, S.R.; Shestakov, N.P. FTIR spectroscopy of early and latewood of *Larix gmelinii* growing along the polar treeline: The correlation between absorption bands and climatic factors. *Wood Mater. Sci. Eng.* **2019**. [CrossRef]
26. Gindl, W. Cell-wall lignin content related to tracheid dimensions in drought sensitive Austrian pine (*Pinus nigra*). *IAWA J.* **2001**, *22*, 113–120. [CrossRef]
27. Fredriksson, M.; Pedersen, N.B.; Thygesen, L.G. The cell wall composition of Norway spruce earlywood and latewood revisited. *Int. Wood Prod. J.* **2018**, *9*, 80–85. [CrossRef]
28. Huang, W.; Hansen, J.K.; Ræbild, A.; Thygesen, L.G.; Bilde, B.; Larsen, J.B. Hvordan påvirkes skovtræarternes vækst af klimaet? [How is the forest tree growth affected by climate?]. *Skoven* **2018**, *10*, 385–387. (In Danish)
29. Holmsgaard, E.; Bang, C. Et træartsforsøg med nåletræer, bøg og eg; de første 10 år [A species trial with conifers, beech and oak; the first 10 years]. *Forstl Forsøgsvæs Dan* **1977**, *35*, 159–196. (In Danish)
30. Callesen, I. Transfer Functions for Carbon Sequestration, Nitrogen Retention and Nutrient Release Capability in Forest Soils Based on Soil Texture Classifications. Ph.D. Thesis, University of Copenhagen, Copenhagen, Denmark, 2003.

31. Harris, I.; Jones, P.D.; Osborn, T.J.; Lister, D.H. Updated high-resolution grids of monthly climatic observations—The CRU TS3.10 Dataset. *Int. J. Climatol.* **2014**, *34*, 623–642. [CrossRef]
32. Thornthwaite, C.W. An approach toward a rational classification of climate. *Geogr. Rev.* **1948**, *38*, 55–94. [CrossRef]
33. Willmott, C.J.; Rowe, C.M.; Mintz, Y. Climatology of the terrestrial seasonal water cycle. *J. Climatol.* **1985**, *5*, 589–606. [CrossRef]
34. Evans, R.; Ilic, J. Rapid prediction of wood stiffness from microfibril angle and density. *For. Prod. J.* **2001**, *51*, 53–57.
35. Lundqvist, S.; Hansson, Å; Olsson, L. SilviScan Measurements on Maritime Pine: French Samples Cut Perpendicular to the Fibres. STFI-Packforsk Report No. 326. Available online: http://www.innventia.com/Documents/Rapporter/STFI-Packforsk%20report%20326.pdf (accessed on 14 February 2019).
36. Ralph, J.; Lundquist, K.; Brunow, G.; Lu, F.; Kim, H.; Schatz, P.F.; Marita, J.M.; Hatfield, R.D.; Ralph, S.A.; Christensen, J.H.; et al. Lignins: Natural polymers from oxidative coupling of 4-hydroxyphenyl- propanoids. *Phytochem. Rev.* **2004**, *3*, 29–60. [CrossRef]
37. Faix, O. Classification of lignins from different botanical origins by FT-IR spectroscopy. *Holzforschung* **1991**, *45*, 21–27. [CrossRef]
38. Schwanninger, M.; Rodrigues, J.C.; Pereira, H.; Hinterstoisser, B. Effects of short-time vibratory ball milling on the shape of FT-IR spectra of wood and cellulose. *Vib. Spectrosc.* **2004**, *36*, 23–40. [CrossRef]
39. Fackler, K.; Stevanic, J.S.; Ters, T.; Hinterstoisser, B.; Schwanninger, M.; Salmén, L. Localisation and characterisation of incipient brown-rot decay within spruce wood cell walls using FT-IR imaging microscopy. *Enzyme Microb. Technol.* **2010**, *47*, 257–267. [CrossRef] [PubMed]
40. Maréchal, Y.; Chanzy, H. The hydrogen bond network in Iβ cellulose as observed by infrared spectrometry. *J. Mol. Struct.* **2000**, *523*, 183–196. [CrossRef]
41. Scheller, H.V.; Ulvskov, P. Hemicelluloses. *Annu. Rev. Plant Biol.* **2010**, *61*, 263–289. [CrossRef] [PubMed]
42. Balakshin, M.; Capanema, E.; Gracz, H.; Chang, H.; Jameel, H. Quantification of lignin-carbohydrate linkages with high-resolution NMR spectroscopy. *Planta* **2011**, *233*, 1097–1110. [CrossRef] [PubMed]
43. Marchessault, R.H. Application of infra-red spectroscopy to cellulose and wood polysaccharides. In Proceedings of the Pure and Applied Chemistry Wood chemistry Symposium, Montreal, QC, Canada, 9–11 August 1961; Volume 5, pp. 107–130. [CrossRef]
44. SAS Institute Ins. *SAS/STAT®14.1 User's Guide*; SAS Institute Inc.: Cary, NC, USA, 2015.
45. Dawson, J.F. Moderation in management research: What, why, when and how. *J. Bus. Psychol.* **2014**, *29*, 1–9. [CrossRef]
46. Gindl, W.; Grabner, M.; Wimmer, R. The influence of temperature on latewood lignin content in treeline Norway spruce compared with maximum density and ring width. *Trees Struct. Funct.* **2000**, *14*, 409–414. [CrossRef]
47. Gindl, W.; Grabner, M. Characteristics of spruce [*Picea abies* (L.) Karst] latewood formed under abnormally low temperatures. *Holzforschung* **2000**, *54*, 9–11. [CrossRef]
48. Kilpeläinen, A.; Peltola, H.; Ryyppö, A.; Sauvala, K.; Laitinen, K.; Kellomäki, S. Wood properties of Scots pines (*Pinus sylvestris*) grown at elevated temperature and carbon dioxide concentration. *Tree Physiol.* **2003**, *23*, 889–897. [CrossRef]
49. Kilpeläinen, A.; Peltola, H.; Ryyppö, A.; Kellomäki, S. Scots pine responses to elevated temperature and carbon dioxide concentration: Growth and wood properties. *Tree Physiol.* **2005**, *25*, 75–83. [CrossRef] [PubMed]
50. Kostiainen, K.; Kaakinen, S.; Saranpää, P.; Sigurdsson, B.D.; Lundqvist, S.O.; Linder, S.; Vapaavuori, E. Stem wood properties of mature Norway spruce after 3 years of continuous exposure to elevated [CO_2] and temperature. *Glob. Chang. Biol.* **2009**, *15*, 368–379. [CrossRef]
51. Donaldson, L.A. Abnormal lignin distribution in wood from severely drought stressed pinus radiata trees. *IAWA J.* **2002**, *23*, 161–178. [CrossRef]
52. Nanayakkara, B.; Lagane, F.; Hodgkiss, P.; Dibley, M.; Smaill, S.; Riddell, M.; Harrington, J.; Cown, D. Effects of induced drought and tilting on biomass allocation, wood properties, compression wood formation and chemical composition of young *Pinus radiata* genotypes (clones). *Holzforschung* **2014**, *68*, 455–465. [CrossRef]

53. Cabane, M.; Afif, D.; Hawkins, S. Lignins and Abiotic Stresses. *Adv. Bot. Res.* **2012**, *61*, 219–262. [CrossRef]
54. Girona, M.M.; Rossi, S.; Lussier, J.-M.; Walsh, D.; Morin, H. Understanding tree growth responses after partial cuttings: A new approach. *PLoS ONE* **2017**, *12*, e0172653. [CrossRef]



© 2019 by the authors. Licensee MDPI, Basel, Switzerland. This article is an open access article distributed under the terms and conditions of the Creative Commons Attribution (CC BY) license (http://creativecommons.org/licenses/by/4.0/).